

Using scanning and transmission electron microscopy to investigate the antibacterial mechanism of action of the medicinal plant *Annona squamosa* Linn.

Achara Dholvitayakhun^a

Nathanon Trachoo^a

Nual-anong Narkkong^b

T.P. Tim Cushnie^{c,*}

^a Faculty of Technology, Mahasarakham University, Khamriang, Kantarawichai, Maha Sarakham 44150, Thailand.

^b Electron Microscopy Unit, Faculty of Science, Mahasarakham University, Khamriang, Kantarawichai, Maha Sarakham 44150, Thailand.

^c Faculty of Medicine, Mahasarakham University, Khamriang, Kantarawichai, Maha Sarakham 44150, Thailand.

Running head: *Annona squamosa* mechanism of action

***Corresponding author:**

Tim Cushnie, Faculty of Medicine, Mahasarakham University, Khamriang, Kantarawichai, Maha Sarakham 44150, Thailand. E-mail: t_cushnie@hotmail.com. Tel.: +66 4375432140 ext. 1159

Highlights

- First study into antibacterial mechanism of action of the medicinal plant *Annona squamosa* Linn.
- Ultrastructure of Gram-positive and Gram-negative pathogens examined following treatment.
- Inhibitory treatments alter peptidoglycan distribution and cause cell wall layers to separate.
- Bactericidal treatments cause malformation of cell wall and leakage of intracellular contents.
- *A. squamosa* disrupts cell wall formation with bacterial death likely to be due to osmotic lysis.

Annona squamosa Linn.



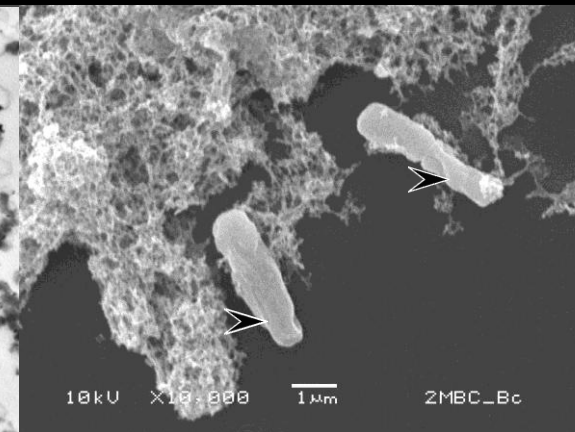
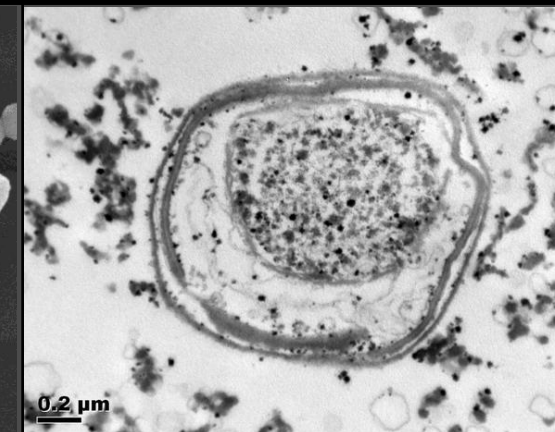
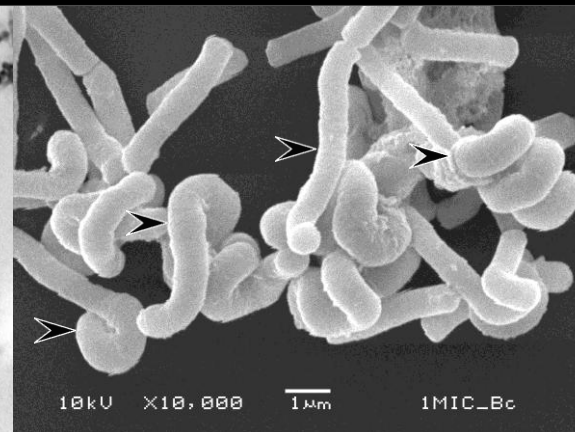
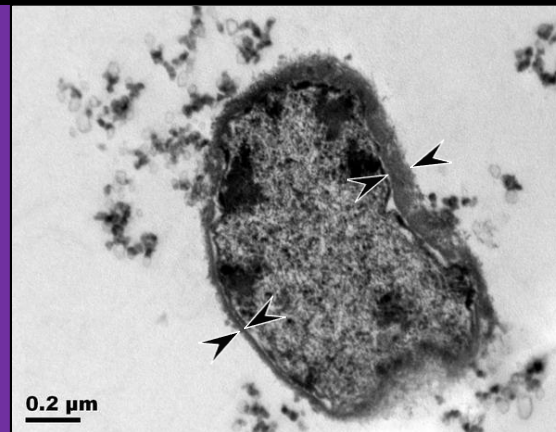
Used to treat dysentery & UTIs, & dress wounds

Inhibitory concentrations cause...

Bactericidal concentrations cause...

Mechanism of action

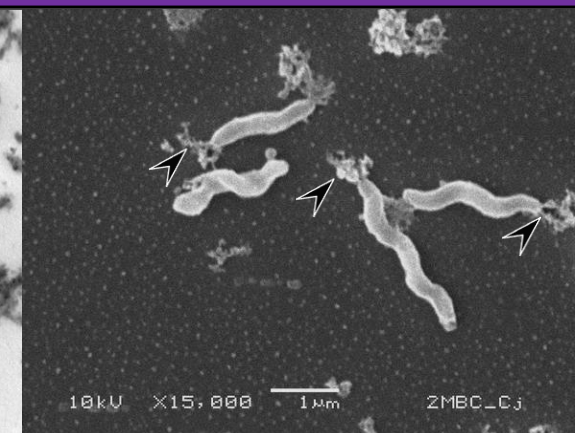
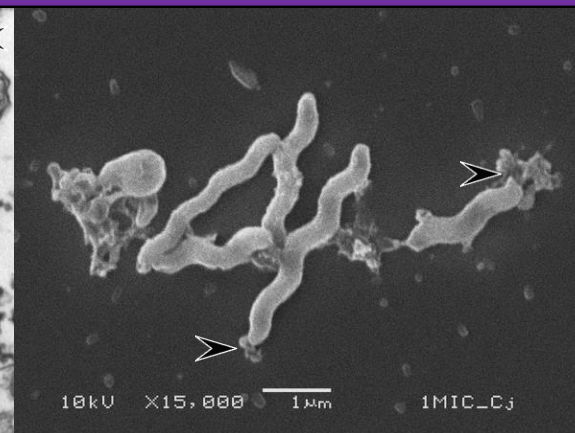
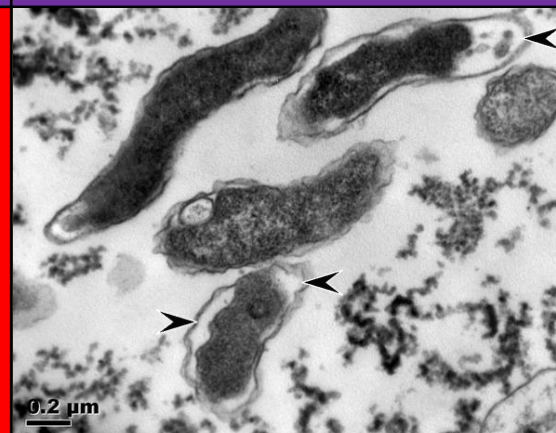
Gram-positive bacteria



Uneven distribution of peptidoglycan; Distortion of cell shape; Cell elongation

Malformed cell walls; Depletion of cytoplasm

Gram-negative bacteria



Separation of cell wall layers; Leakage of intracellular contents

Leakage of intracellular contents; Depletion of cytoplasm

- Bacterial growth inhibition involves the disruption of cell wall formation
- Bacterial death is likely to be due to loss of the wall's mechanical strength & osmotic lysis
- Further studies are now needed to identify the molecular targets of *A. squamosa*

ABSTRACT

Leaves of *Annona squamosa* Linn. (Annonaceae), used in traditional medicine for infection treatment and prevention, have been shown to possess antibacterial activity in several recent studies. We examined the effect of the active reticuline-containing fraction of this traditional medicine on bacterial cell ultrastructure to gain insight into its mechanism of action. *Bacillus cereus* and *Campylobacter jejuni* were used as representative species of Gram-positive and Gram-negative pathogen. Time-kill assays were performed with each bacterial species and 1xMIC (minimum inhibitory concentration), 2xMIC, 1xMBC (minimum bactericidal concentration) and 2xMBC levels of *A. squamosa* extract to identify treatment times and concentrations at which inhibitory and bactericidal effects occur. Treated bacteria were then examined by scanning and transmission electron microscopy. In *B. cereus* populations treated with inhibitory concentrations of extract, peptidoglycan distribution was altered, cell shape was distorted, and cells were up to 6.9 times their normal length. Inhibitory concentrations caused no changes in *C. jejuni* cell shape or length, but separation of the cell wall layers was observed together with leakage of intracellular contents. In *B. cereus* and *C. jejuni* populations treated with bactericidal concentrations of extract, the cell envelope was compromised and the cytoplasm depleted. These results suggest *A. squamosa* extract inhibits bacterial growth by disrupting peptidoglycan formation, with cell death probably occurring due to loss of the wall's mechanical strength and osmotic lysis.

Keywords: medicinal plant; antibacterial; alkaloid; reticuline; mechanism; mode

1. Introduction

Antibiotic resistance is a major global problem. For patients infected with drug-resistant bacteria, mortality rates are twice as high, hospital stays are twice as long, and healthcare costs are greatly increased compared to infections with drug-sensitive strains (French, 2010; WHO, 2012). Alarming, the situation is set to get worse (Livermore, 2012). Increasing antibiotic production and consumption in newly prosperous developing countries is expected to accelerate the emergence of drug-resistant bacterial strains (Livermore, 2012). Also, increasing population movement and displacement through leisure travel, medical tourism and climate change is expected to accelerate the spread of resistance (Gould, 2010; van der Bij and Pitout, 2012). A third cause for concern is the dwindling antibiotic pipeline (Laxminarayan et al., 2013). Following the failure of genomics-based discovery, a strategy widely adopted by the pharmaceutical industry in the 1990s, there are now very few prospective new drugs to replace those losing efficacy (Laxminarayan et al., 2013). In recognition of this growing threat to public health, the World Health Organization has called for urgent corrective action including the development of new antibacterial therapies (WHO, 2012).

Natural products, in the form of standardized extracts or isolated compounds, represent an important source of chemical diversity and a potential source of new treatments and drug leads (Dubey and Padhy, 2013). Medicinal plants are a particularly attractive starting point for these discovery efforts because, unlike most other natural product sources, they can be rationally selected for antibacterial testing based on traditional use (Emeka et al., 2012; Zadra et al., 2013). Robust and sustained research programmes are needed to ascertain efficacy and safety though. According to Ríos & Recio (2005), many researchers view the antimicrobial activity of medicinal plants as merely a complement to their studies, without ever determining the plant's real therapeutic potential. An important step in the development of any new evidence-based antibacterial treatment is the elucidation of its mechanism of action i.e. identification of the cellular function the agent inhibits and the cellular structure the agent binds to. Resolution of these details permits anticipation of problems relating to clinical safety and bacterial resistance (Payne et al., 2007; Silver, 2011), as well as understanding of synergistic and antagonistic drug interactions (Acar, 2000; Auerbach et al., 2010).

Annona squamosa Linn. (Annonaceae), commonly known as 'sugar apple', is a small deciduous tree widely distributed in South America, the Caribbean, Australasia, and Indomalaya. *A. squamosa* leaves are used as a decoction to treat dysentery and urinary tract infections in traditional Indian, Thai, and American medicine (Rueangrangi and Mangkhakhup, 2004; Umadevi et al., 2011; Yusha'u et al., 2011). The leaves are also crushed and applied to wounds in traditional Indian medicine (Pandey and Barve, 2011). Studies by Dholvitayakhun et al. (2013), Shokeen et al. (2005), and Yusha'u et al. (2011) confirm that *A. squamosa* leaf extract has antibacterial activity *in vitro*, with susceptible organisms including *Neisseria gonorrhoeae*, *Campylobacter jejuni*, *Staphylococcus aureus*, *Streptococcus pneumoniae*, *Bacillus cereus*, and *Listeria monocytogenes*. Antibacterial activity of the traditional medicine has been at least partially attributed to the alkaloid reticuline, but no information is available on the underlying mechanism of action. In the present study, we investigate how *A. squamosa* exerts its antibacterial effect by analysing the changes that inhibitory and bactericidal concentrations of the medicinal plant induce in the ultrastructure of Gram-positive and Gram-negative bacteria.

2. Materials and methods

2.1 Bacteria

Bacillus cereus ATCC 11778 and *Campylobacter jejuni* ATCC 29428, obtained from the American Type Culture Collection, were used as representative species of Gram-positive and Gram-negative bacteria. Prior to testing, *B. cereus* was cultured on Mueller-Hinton agar (Criterion, USA) and incubated at 37°C for 24 h under aerobic conditions. *C. jejuni* was cultured on brucella agar supplemented with 62.5 mg/l each of ferrous sulphate, sodium metabisulfite and sodium pyruvate (Criterion). Incubation was at 42°C for 48 h under microaerobic conditions (5% O₂, 10% CO₂, and 85% N₂). Inocula were prepared by suspending bacterial colonies in 0.1% (w/v) sterile peptone water, and enumeration graphs were used to achieve a final cell density of 5 x 10⁵ cfu/ml in all assays.

2.2 Processing of the plant material

Fresh leaves of *A. squamosa* were collected in Maha Sarakham, Thailand in September 2009. Species identity was confirmed by Ms. Suttira Khumkratok of the Walai Rukhvej Botanical Research Institute (Thailand), and a voucher specimen was deposited (Achara 03-10). The leaves were processed using previously described protocols (Dholvitayakhun et al., 2013) as summarized below. Leaves were initially rinsed and sliced, then dried in a hot air oven (50°C; FD240; Franz Binder GmbH, Germany) for 24 h, and ground and sieved with 80 mesh stainless steel sieves. The powdered leaves were added [1:10 (w/v)] to 95% (v/v) ethanol (VWR International Ltd., UK) and shaken at 120 rpm (25°C) for 24 h (PSU 5T Plus; BioScan Ltd., Russia), prior to filtration, rotary evaporation (50°C; Rotavapor R-12 V-700/V-850, Büchi Labortechnik AG, Switzerland), and lyophilization (PowerDry PL 3000; Heto Lab Equipment, USA). The resulting ethanol extract was subjected to silica gel column chromatography, using a 4x60 cm column packed with silica gel 60 (63-200 µm; Merck, Germany) and eluting with an increasing polarity gradient (ethanol:hexane) at a flow rate of 3 ml/min. This yielded eight fractions. Bioactivity testing and subsequent LC/DAD-APCI/MS analysis (Agilent Technologies 1100 series, USA) of these fractions indicated antibacterial activity was concentrated in the reticuline-containing fraction (Dholvitayakhun et al., 2013). In total, 17.3 g crude ethanol extract was obtained from 200 g dried leaf material, and 4.75 g of the antibacterial reticuline-containing fraction was obtained following gradient elution column chromatography of 10 g of the crude ethanol extract. All subsequent assays were performed with the reticuline-containing fraction. This was stored in a tightly sealed, foil-wrapped bottle at 4°C until required. DMSO (Honeywell International Inc., Germany) was used to dissolve the extract for time-kill and electron microscopy studies, the final concentration of solvent being 2% (v/v) in all assays.

2.3 Time-kill studies

Time-kill assays were performed with *A. squamosa* extract and the two test species of bacteria to identify suitable treatment times and concentrations for electron microscopy studies. For assays with *B. cereus*, Mueller-Hinton broth (Criterion) was used as the growth medium, while for assays with *C. jejuni*, Mueller-Hinton broth containing 5% (v/v) laked sheep blood (National Laboratory Animal

Centre, Mahidol University, Thailand) was used. Sterile glass flasks containing 20 ml growth medium only, 20 ml growth medium supplemented with 2% (v/v) DMSO, and 20 ml growth medium supplemented with extract were inoculated with either *B. cereus* or *C. jejuni* (final cell density: $\sim 5 \times 10^5$ cfu/ml bacteria; CLSI, 1999). Extract was tested at 1xMIC (minimum inhibitory concentration), 2xMIC, 1xMBC (minimum bactericidal concentration) and 2xMBC levels determined previously (Dholvitayakhun et al., 2013). This equated to 125 $\mu\text{g/ml}$ (1xMIC), 250 $\mu\text{g/ml}$ (2xMIC), 500 $\mu\text{g/ml}$ (1xMBC) and 1000 $\mu\text{g/ml}$ (2xMBC) for *B. cereus*, and 250 $\mu\text{g/ml}$ (1xMIC), 500 $\mu\text{g/ml}$ (2xMIC and 1xMBC) and 1000 $\mu\text{g/ml}$ (2xMBC) for *C. jejuni* (Dholvitayakhun et al., 2013). Inoculated flasks were incubated with shaking (100 rpm) at either 42°C under microaerobic conditions for *C. jejuni* or 37°C under aerobic conditions for *B. cereus*. Viable counts were performed for each suspension after various time intervals (0, 1, 2, 4, 8, 12 and 24 h for *B. cereus*, and 0, 2, 4, 12 and 24 h for *C. jejuni*) by removing 1 ml samples, preparing a dilution series in 0.1% (w/v) sterile peptone water (10^{-1} - 10^{-6}) and plating out this dilution series (ten 20 μl drops per dilution) on agar. Time-kill assays were performed in duplicate to verify the reproducibility of results.

2.4 Preparation of specimens for electron microscopy

For electron microscopy studies, Mueller-Hinton broth was used as the growth medium for *B. cereus*, and Mueller-Hinton broth containing 5% (v/v) laked sheep blood was used as the growth medium for *C. jejuni*. Sterile glass flasks containing 40 ml growth medium only, 40 ml growth medium supplemented with 2% (v/v) DMSO, and 40 ml growth medium supplemented with fractionated extract were inoculated so as to contain $\sim 5 \times 10^5$ cfu/ml bacteria. The rationale for including growth medium with and without DMSO in the study design was to rule out the possibility that the solvent itself might induce ultrastructural changes in the bacterial cells. Both test species, *B. cereus* and *C. jejuni*, were treated with 1xMIC and 2xMBC levels of the fraction. Flasks of *B. cereus* were incubated at 37°C under aerobic conditions for a period of 12 h, while flasks of *C. jejuni* were incubated at 42°C under microaerobic conditions for a period of 4h. Bacterial cells were collected by centrifugation at 6000 rpm at 4°C for 10 min. The pellets were fixed overnight with 2.5% (w/v) glutaraldehyde in 0.1 M phosphate buffered saline (PBS; pH 7.2) at 4°C. These reagents and all subsequent reagents were

obtained from Electron Microscopy Sciences (USA). After fixation, cells were washed three times with 1 ml of PBS (each time for 10 min), and post-fixed with 1% (w/v) osmium tetroxide in PBS for 1 h. Cells were then washed three times with 1 ml distilled water (each time for 10 min) and *en bloc* stained in the dark with 5% (w/v) uranyl acetate for 1 h. This was followed by three further washes with 1 ml distilled water (each time for 10 min). The cells were then dehydrated through suspension in increasing concentrations of aqueous acetone solution [20%, 40%, 60%, 80%, and 100% (v/v); twice at 100% (v/v)]. Cells were centrifuged at 2500 rpm at 4°C for 5 min between each of these dehydration steps.

2.5 Scanning electron microscopy (SEM)

After dehydration in acetone, three 25 μ l samples of each suspension were withdrawn and applied to the surface of three cover slips. These specimens were allowed to air-dry, then coated with gold using a sputter coater (SPI module, Structure Probe Inc., USA). Morphology of the bacterial cells was examined using a scanning electron microscope (JSM-6460LV, JEOL Ltd., Japan), and bacterial cell length was determined using ImageJ 1.46 software (National Institutes of Health, USA). The cell lengths of the DMSO only-treated bacteria were compared with those of the three other treatment groups by one way analysis of variance (ANOVA) in completely randomized design (CRD) using SPSS software version 11.5 (SPSS Inc., USA). *P* values less than 0.05 were considered significant.

2.6 Transmission electron microscopy (TEM)

Following acetone dehydration, the pellet of cells was suspended in a 1:1 ratio of acetone and epoxy resin overnight, then fresh 100% (v/v) epoxy resin for 3 h. These samples were embedded in Epon 812 and polymerized in a hot air oven at 60°C for 24 h. The resin embedded pellet was then sectioned on an ultramicrotome (MTX, RMC products, USA) with a diamond knife. The thin sections were placed on copper grids and stained with 0.4% (w/v) lead citrate for 15 min prior to examination with a transmission electron microscope (JEM 1230, JEOL Ltd., Japan).

3. Results

3.1 Time-kill studies with *B. cereus* and *C. jejuni*

A. squamosa extract exerted a concentration-dependent effect against both bacterial species (Fig. 1). Bactericidal activity [i.e. a 99.9% decrease in bacterial viability (CLSI, 1999)] was first noted against *B. cereus* at a concentration of 2xMBC and treatment time of 12 h (Fig. 1a), and against *C. jejuni* at a concentration of 2xMBC at 4 h (Fig. 1b). These concentrations and treatment times were selected for use in subsequent SEM and TEM studies seeking to understand how *A. squamosa* kills bacteria. *A. squamosa* was also tested at 1xMIC to establish how bacterial growth is inhibited and obtain a clearer picture of the antibacterial mechanism of action.

3.2 SEM and TEM analysis of treated and untreated *B. cereus*

SEM examination of DMSO only-treated (control) *B. cereus* confirmed these cells had not been injured by the DMSO or subsequent processing. The bacteria were uniformly rod-shaped in their morphology, they had typical dimensions and a smooth cell surface, and were present in large numbers (Fig. 2a). TEM analysis showed their cell wall and cytoplasmic membrane were intact (Fig. 2b; arrows), and their cytoplasm was homogeneously electron dense (Fig. 2b). Comparison of these DMSO-only treated bacteria and the control cells incubated without DMSO confirmed there were no differences in ultrastructure (data not shown) or cell length (Fig. 3).

Samples of *B. cereus* treated with 1xMIC *A. squamosa* extract had a very different appearance. These cells were significantly elongated (up to 6.9-fold longer than control cells; Fig. 2c and Fig. 3; $p=0.001$), many having a twisted or helical appearance (Fig. 2c; arrows). TEM analysis indicated that peptidoglycan was unevenly distributed in the bacterial cell wall (Fig. 2d; arrows). Also, partial loss of cytoplasmic electron density was noted in some cells (Fig. 2d).

Very few intact cells were detected in samples of *B. cereus* treated with 2xMBC *A. squamosa* extract. Of the few intact or semi-intact cells that were observed, some were elongated (up to 5.7-fold longer; Fig. 3), though mean size overall was not significantly affected ($p=0.058$). Some of the cells had visibly malformed cell walls (Fig. 2e; arrows), and most were surrounded by large quantities of electron dense material (Fig. 2e). It can be seen from TEM analysis (Fig. 2f) that the cell wall was

thinner than in control cells, the cytoplasmic membrane was compromised (arrow), and there was almost complete loss of cytoplasmic electron density. As with the SEM examination, large quantities of electron dense extracellular material were detected (Fig. 2f).

3.3 SEM and TEM analysis of treated and untreated *C. jejuni*

SEM analysis of *C. jejuni* treated with DMSO only (control) revealed large numbers of cells with normal spiral-shaped morphology and typical dimensions (Fig. 4a). TEM examination of cells indicated their cytoplasm was homogeneously electron dense (Fig. 4b). Also, the Gram-negative cell envelope appeared normal. All three layers were discernible (Fig. 4b; arrows), except at the twist in the mid-section of the cell, which was not flush with the plane of the specimen. Similar results were obtained for control cells incubated without DMSO.

In samples of *C. jejuni* treated with 1xMIC *A. squamosa* extract, the cells all had a normal shape (Fig. 4c). Cells were examined for elongation by determining the total length of the helix (as opposed to the shortest distance between poles) but no elongation was detected (Fig. 3 and 4c). SEM analysis did show leakage of intracellular material from some cells though (Fig. 4c; arrows). This was accompanied by partial loss of cytoplasmic electron density in some cells, and the appearance of electron dense material outside the cells (Fig. 4d). Separation of the layers of the cell wall was also detected (Fig. 4d; arrows).

Very few intact cells were detected in samples of *C. jejuni* treated with 2xMBC *A. squamosa* extract. Leakage was observed in those cells that could be seen (Fig. 4e; arrows). Cells examined by TEM showed partial to complete loss of electron density of both their cell envelope and cytoplasm (Fig. 4f). In addition, large quantities of electron dense extracellular material were observed (Fig. 4f).

4. Discussion

A. squamosa leaves are used in different indigenous medical systems for wound care and the treatment of infection. We investigated the mechanism of action of this traditional medicine with a view to facilitating its development as a modern, evidence-based antibacterial therapy. In the absence of any previous studies or hypotheses regarding the plant's mechanism of action, electron microscopy was

used to determine the global effect of *A. squamosa* on bacterial cells. SEM yields information on how antibacterial agents affect the overall morphology and surface characteristics of bacterial cells, while TEM provides information on how the internal architecture of cells is affected. Used together, these techniques can give valuable insight into the antibacterial mechanism of action of novel antibacterial agents (Suk et al., 2010; Suwalak and Voravuthikunchai, 2009). Taking into consideration the structural differences that exist between the Gram-positive and Gram-negative cell envelope and the possibility *A. squamosa* might affect these differently, representative species of each cell type were examined.

Results from the present investigation show that when Gram-positive *B. cereus* is treated with inhibitory concentrations of *A. squamosa* extract, the cells become twisted and sometimes helical in shape (Fig. 2c). This strongly suggests that *A. squamosa* disrupts cell wall formation, since bacterial shape is governed by the peptidoglycan sacculus (Vollmer et al., 2008). It is not possible to pinpoint the cellular target(s) from our data, but the observation of elongated bacteria lacking septa (Fig. 2c and Fig. 3) and bacteria with an uneven distribution of peptidoglycan (Fig. 2d) suggests *A. squamosa* may be interfering with the membrane proteins EzrA and GpsB. These proteins co-ordinate formation of peptidoglycan in the lateral cell wall (cell elongation) and septal wall (cell division) during cell cycle progression. EzrA recruits peptidoglycan-synthesizing PBP enzymes to the site of cell division, and GpsB directs these enzymes to the cylindrical part of the cell following cell division (Claessen et al., 2008). Other possible targets include the membrane-associated cytoskeletal proteins MreB and FtsZ. These proteins form the scaffolding required for cell division and elongation, providing topological information to the PBP enzymes (Adams and Errington, 2009; Shaevitz and Gitai, 2010). Recent work with berberine and sanguinarine, alkaloids structurally related to reticuline, suggest these act on FtsZ (Cushnie et al., 2014). In the present study, treatment of *B. cereus* with bactericidal concentrations of *A. squamosa* left very few of the bacterial cells intact. Those cells that could be seen had malformed cell walls (Fig. 2e and 2f), their cytoplasm was less electron dense (Fig. 2f), and they were surrounded by large quantities of extracellular detritus (Fig. 2e and 2f). These results suggest high concentrations of extract disrupt cell wall formation to such an extent that its mechanical strength

is lost and the cell undergoes osmotic lysis. The extracellular detritus observed in Figs. 2e and 2f is likely to be cytoplasmic material from the lysed cells.

When Gram-negative *C. jejuni* was treated with inhibitory concentrations of *A. squamosa* extract, the layers of its cell wall became separated (Fig. 4d). This represents further evidence that *A. squamosa* disrupts formation of the peptidoglycan sacculus. Normally, the outer membrane and peptidoglycan layer of the Gram-negative cell wall are firmly linked by Braun's lipoprotein, but the lipoprotein requires a properly formed peptidoglycan layer to anchor itself to. Unlike *B. cereus*, cell shape and length were unaltered in extract-treated *C. jejuni* (Fig. 3 and Fig. 4c). This difference in results may reflect the fact that Gram-negative bacteria have a much thinner layer of peptidoglycan than Gram-positive bacteria. In some Gram-negative bacteria, the cell wall contains just a monolayer of peptidoglycan (Singleton, 1999), so disruption of its synthesis could result in osmotic lysis before any changes in cell shape or length occur. This interpretation of results is supported by two findings. Firstly, our observation of leaking intracellular contents (Fig. 4c) accompanied by a decrease in the electron density of the cytoplasm (Fig. 4d) and the appearance of electron dense material outside the cell (Fig. 4d) confirms that, even at inhibitory concentrations, *A. squamosa* extract induces lysis in a number of cells. Secondly, our previous finding that the MBC of *A. squamosa* extract against *C. jejuni* is just 2-fold higher than the MIC (Dholvitayakhun et al., 2013), is indicative of a mechanism of action in which inhibition of cell growth is very quickly followed by cell death. After treatment with bactericidal concentrations of *A. squamosa*, very few intact *C. jejuni* cells were observed. Leakage of intracellular contents was seen (Fig. 4e), together with a decrease in cell envelope and cytoplasm electron density (Fig. 4f), and the appearance of large quantities of extracellular detritus (Fig. 4f). As with *B. cereus*, these images suggest high concentrations of extract reduce the cell wall's mechanical strength below the limit needed to withstand osmotic lysis.

5. Conclusion

In conclusion, our study suggests that *A. squamosa* leaf extract exerts its antibacterial effect by disrupting cell wall formation. The precise cellular target(s) remain unknown but may include those bacterial proteins responsible for coordinating peptidoglycan formation in the lateral and septal cell

wall, or the cytoskeletal proteins that provide topological information to the peptidoglycan-synthesizing PBP enzymes. These findings help justify the case for further investigation of *A. squamosa* (e.g. toxicity studies) and pave the way for more focused mechanism of action studies employing genetic and molecular techniques (e.g. target overexpression and size-exclusion chromatography).

Acknowledgements

This work was supported by the Office of the Higher Education Commission, Ministry of Education, Thailand, through a CHE PhD scholarship. The authors report no conflicts of interest. The authors are very grateful to Ms. Suttira Khumkratok (Walai Rukhavej Botanical Research Institute) for identifying the plant material and assisting with voucher specimen preparation. They would also like to thank Asst. Prof. Dr. Uthai Sakee (Mahasarakham University) for chemistry advice, and Ms. Thatsawan Inthasoi (Rajamangala University of Technology Lanna Tak) for assistance with statistics.

References

- Acar JF. Antibiotic synergy and antagonism. *Med Clin N Am* 2000; 84:1391-406.
- Adams DW, Errington J. Bacterial cell division: assembly, maintenance and disassembly of the Z ring. *Nat Rev Microbiol* 2009; 7:642-53.
- Auerbach T, Mermershtain I, Davidovich C, Bashan A, Belousoff M, Wekselman I et al. The structure of ribosome-lankacidin complex reveals ribosomal sites for synergistic antibiotics. *Proc Natl Acad Sci* 2010; 107:1983-8.
- Claessen D, Emmins R, Hamoen LW, Daniel RA, Errington J, Edwards DH. Control of the cell elongation-division cycle by shuttling of PBP1 protein in *Bacillus subtilis*. *Mol Microbiol* 2008; 68:1029-46.
- CLSI. Methods for determining bactericidal activity of antimicrobial agents; Approved guideline (M26-A). Wayne (PA): Clinical and Laboratory Standards Institute; 1999.
- Cushnie TPT, Cushnie B, Lamb AJ. Alkaloids: An overview of their antibacterial, antibiotic-enhancing and antivirulence activities. *Int J Antimicrob Ag* 2014; 44:377-86.
- Dholvitayakhun A, Trachoo N, Sakee U, Cushnie TPT. Potential applications for *Annona squamosa* leaf extract in the treatment and prevention of foodborne bacterial disease. *Nat Prod Commun* 2013; 8:385-8.
- Dubey D, Padhy RN. Antibacterial activity of *Lantana camara* L. against multidrug resistant pathogens from ICU patients of a teaching hospital. *J Herb Med* 2013; 3:65-75.
- Emeka PM, Badger-Emeka LI, Fateru F. *In vitro* antimicrobial activities of *Acalypha ornate* leaf extracts on bacterial and fungal clinical isolates. *J Herb Med* 2012; 2:136-42.
- French GL. The continuing crisis in antibiotic resistance. *Int J Antimicrob Ag* 2010; 36:S3-S7.
- Gould IM. Coping with antibiotic resistance: the impending crisis. *Int J Antimicrob Ag* 2010; 36:S1-S2.
- Laxminarayan R, Duse A, Wattal C, Zaidi AKM, Wertheim HFL, Sumpradit N et al. Antibiotic resistance-the need for global solutions. *Lancet Infect Dis* 2013; 13:1057-98.
- Livermore DM. Fourteen years in resistance. *Int J Antimicrob Ag* 2012; 39:283-94.

- Pandey N, Barve D. Phytochemical and pharmacological review on *Annona squamosa* Linn. Int J Res Pharm and Biomed Sci 2011; 2:1404-12.
- Payne DJ, Gwynn MN, Holmes DJ, Pompliano DL. Drugs for bad bugs: confronting the challenges of antibacterial discovery. Nat Rev Drug Discov 2007; 6:29-40.
- Ríos JL, Recio MC. Medicinal plants and antimicrobial activity. J Ethnopharmacol 2005; 100:80-4.
- Rueangrangi N, Mangkhakhup T. Thai herbs (Vol. 1). Bangkok: Bi Hen Ti; 2004.
- Shaevitz JW, Gitai Z. The structure and function of bacterial actin homologs. Cold Spring Harb Perspect Biol 2010; 2.
- Shokeen P, Ray K, Bala M, Tandon V. Preliminary studies on activity of *Ocimum sanctum*, *Drynaria quercifolia*, and *Annona squamosa* against *Neisseria gonorrhoeae*. Sex Transm Dis 2005; 32:106-11.
- Silver LL. Challenges of antibacterial discovery. Clin Microbiol Rev 2011; 24:71-109.
- Singleton P. Bacteria in biology, biotechnology and medicine. Chichester: John Wiley and Sons Ltd; 1999.
- Suk KT, Kim HS, Kim MY, Kim JW, Uh Y, Jang IH et al. *In vitro* antibacterial and morphological effects of the urushiol component of the sap of the Korean lacquer tree (*Rhus vernicifera* Stokes) on *Helicobacter pylori*. J Korean Med Sci 2010; 25:399-404.
- Suwalak S, Voravuthikunchai SP. Morphological and ultrastructural changes in the cell structure of enterohaemorrhagic *Escherichia coli* O157:H7 following treatment with *Quercus infectoria* nut galls. J Electron Microsc 2009; 58:315-20.
- Umadevi KJ, Vanitha V, Vijayalakshmi K. Antimicrobial activity of three Indian medicinal plants - an *in vitro* study. The Bioscan 2011; 6:25-8.
- Van der Bij AK, Pitout JDD. The role of international travel in the worldwide spread of multiresistant Enterobacteriaceae. J Antimicrob Chemoth 2012; 67:2090-100.
- Vollmer W, Blanot D, De Pedro MA. Peptidoglycan structure and architecture. FEMS Microbiol Rev 2008; 32:149-67.
- WHO. The evolving threat of antimicrobial resistance: options for action. Geneva: World Health Organization; 2012.

Yusha'u M, Taura DW, Bello B, Abdullahi N. Screening of *Annona squamosa* extracts for antibacterial activity against some respiratory tract isolates. *Int Res Pharm Pharmacol* 2011; 1:237-41.

Zadra M, Piana M, Boligon AA, De Brum TF, Rossato LL, Alves SH et al. *In vitro* evaluation of the antimicrobial and antimycobacterial activities of *Solanum guaraniticum* A. St.-Hil. leaves. *J Appl Pharm Sci* 2013; 3:19-23.

Figure 1 The effect of fractionated *A. squamosa* extract on populations of $\sim 5 \times 10^5$ cfu/ml (a) *B. cereus* ATCC 11778 and (b) *C. jejuni* ATCC 29428 (error bars represent standard deviation of the mean of ten samples). \diamond : growth medium only; \bullet : 2% (v/v) DMSO; \blacktriangle : 1xMIC extract; \square : 2xMIC extract; \triangle : 1xMBC extract; \blacksquare : 2xMBC extract; ---: minimum detectable number of bacteria.

Figure 2 Images of *B. cereus* ATCC 11778 obtained by SEM (a, c & e; scale bar = 1 μ m) and TEM (b, d, & f; scale bar = 0.2 μ m) following treatment with 2% (v/v) DMSO (control; a & b), 1xMIC extract (c & d) and 2xMBC extract (e & f). Arrowheads indicate the location of the cytoplasmic membrane (CM) and cell wall (W) in control cells (image b), the location of treated cells with an elongated and twisted / helical appearance (image c), treated cells with an uneven distribution of peptidoglycan in their cell wall (image d), and treated cells with malformed cell walls (image e) and compromised cytoplasmic membrane (image f).

Figure 3 Minimum, maximum, and mean cell length of *B. cereus* ATCC 11778 (grey bars) and *C. jejuni* ATCC 29428 (black bars) following treatment with 1xMIC and 2xMBC levels of fractionated *A. squamosa* extract (error bars represent standard deviation of the mean length of 15-30 cells). * indicates p value < 0.05

Figure 4 Images of *C. jejuni* ATCC 29428 obtained by SEM (a, c & e; scale bar = 1 μ m) and TEM (b, d & f; scale bar = 0.2 μ m) following treatment with 2% (v/v) DMSO (control; a & b), 1xMIC extract (c & d) and 2xMBC extract (e & f). Arrowheads indicate the location of the outer membrane (OM), periplasmic space and peptidoglycan (P) and cytoplasmic membrane (CM) in control cells (image b), and treated cells exhibiting leakage (images c & e) and separation of the cell wall layers (image d).

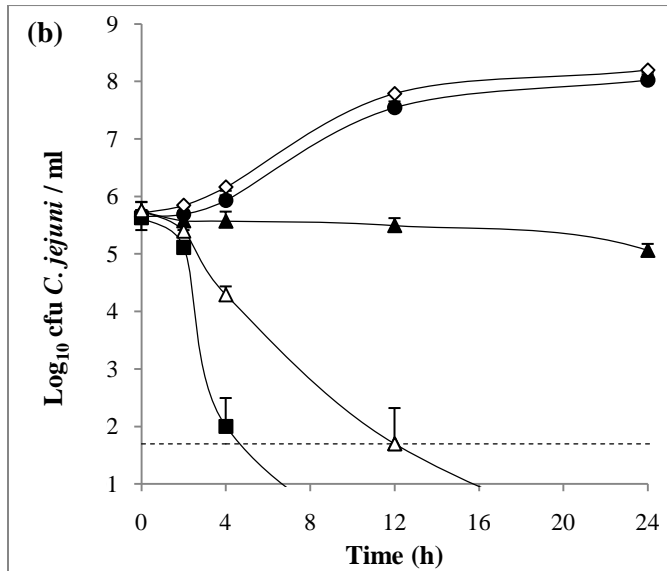
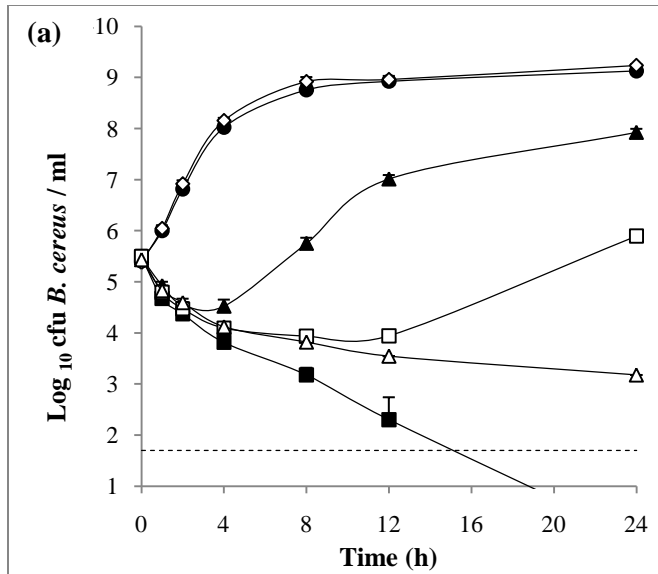


Figure 1 The effect of fractionated *A. squamosa* extract on populations of $\sim 5 \times 10^5$ cfu/ml (a) *B. cereus* ATCC 11778 and (b) *C. jejuni* ATCC 29428 (error bars represent standard deviation of the mean of ten samples). ◇: growth medium only; ●: 2% (v/v) DMSO; ▲: 1xMIC extract; □: 2xMIC extract; △: 1xMBC extract; ■: 2xMBC extract; ---: minimum detectable number of bacteria.

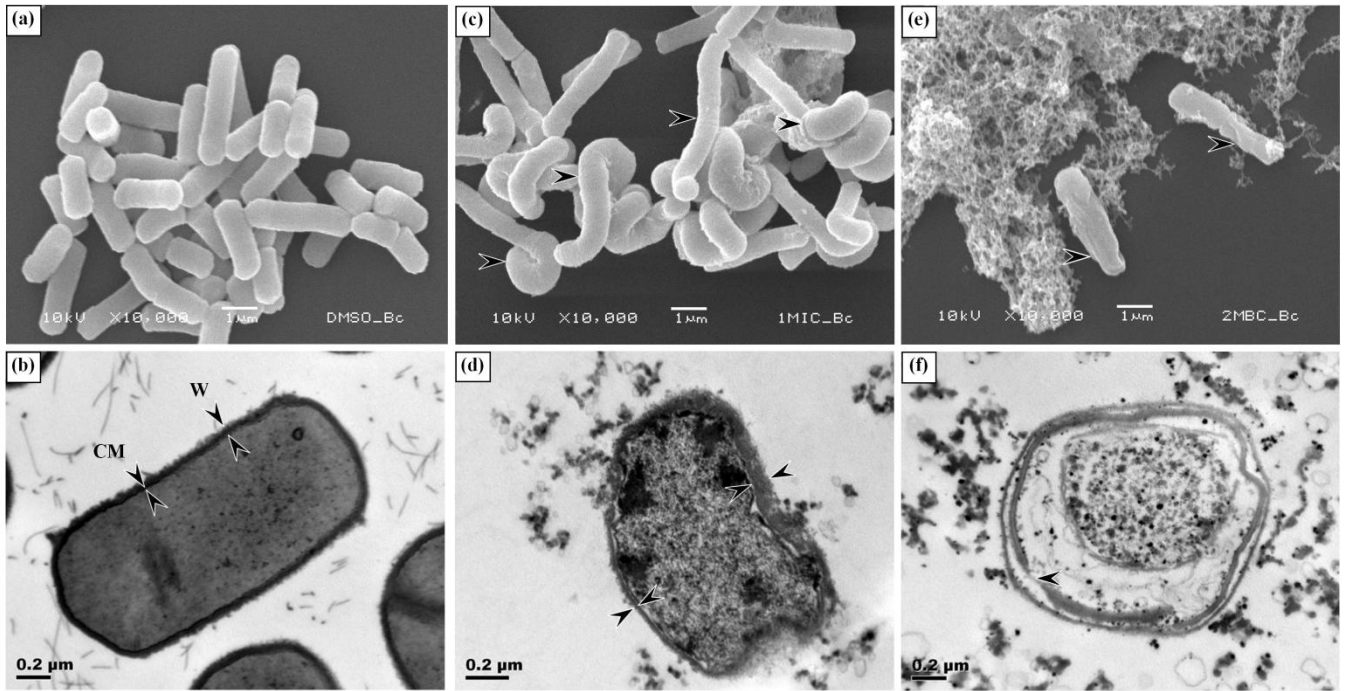


Figure 2 Images of *B. cereus* ATCC 11778 obtained by SEM (a, c & e; scale bar = 1 μm) and TEM (b, d, & f; scale bar = 0.2 μm) following treatment with 2% (v/v) DMSO (control; a & b), 1xMIC extract (c & d) and 2xMBC extract (e & f). Arrowheads indicate the location of the cytoplasmic membrane (CM) and cell wall (W) in control cells (image b), the location of treated cells with an elongated and twisted / helical appearance (image c), treated cells with an uneven distribution of peptidoglycan in their cell wall (image d), and treated cells with malformed cell walls (image e) and compromised cytoplasmic membrane (image f).

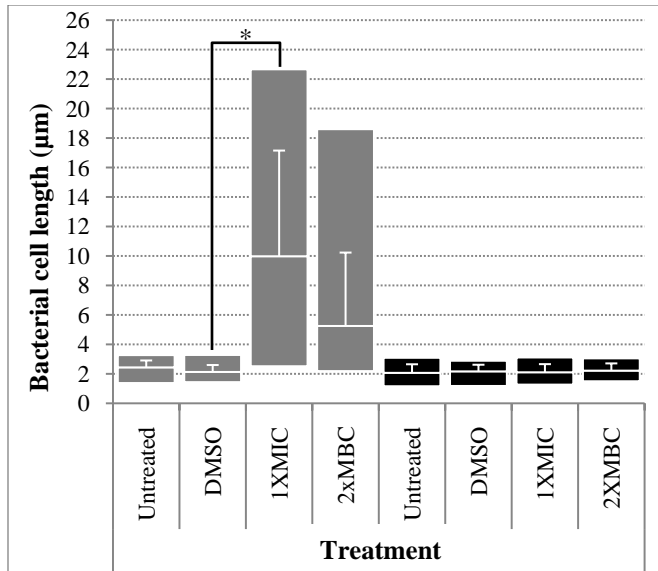


Figure 3 Minimum, maximum, and mean cell length of *B. cereus* ATCC 11778 (grey bars) and *C. jejuni* ATCC 29428 (black bars) following treatment with 1xMIC and 2xMBC levels of fractionated *A. squamosa* extract (error bars represent standard deviation of the mean length of 15-30 cells). * indicates p value <0.05

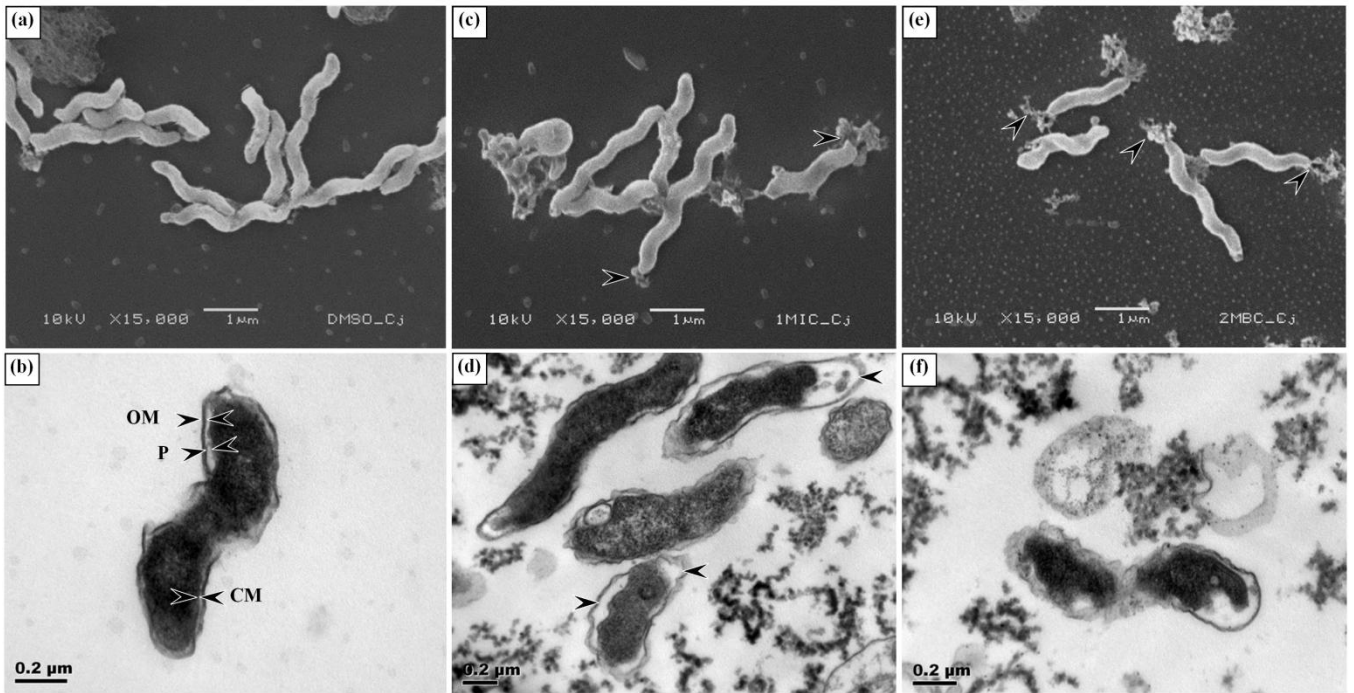


Figure 4 Images of *C. jejuni* ATCC 29428 obtained by SEM (a, c & e; scale bar = 1 μm) and TEM (b, d & f; scale bar = 0.2 μm) following treatment with 2% (v/v) DMSO (control; a & b), 1xMIC extract (c & d) and 2xMBC extract (e & f). Arrowheads indicate the location of the outer membrane (OM), periplasmic space and peptidoglycan (P) and cytoplasmic membrane (CM) in control cells (image b), and treated cells exhibiting leakage (images c & e) and separation of the cell wall layers (image d).